ELSEVIER

Spectral analysis of the $4d^9 6s$ configuration in eight times ionized xenon, Xe IX

M. Raineri*, M. Gallardo, J.G. Reyna Almandos

Centro de Investigaciones Opticas (CIOp), Casilla de Correo 124, 1900 La Plata, Argentina

Abstract

A capillary light source was used to observe the spectrum of eight times ionized xenon, Xe IX, in the vacuum ultraviolet range, 270–2000 Å. Sixteen transitions have been identified as combinations between energy levels of the $4d^9 6s$ with $4d^9 5p$ configuration, and all $4d^9 6s$ levels have been determined. The present analysis is based on an accurate extrapolation of energy parameters and experimental energy level values in the Pd I isoelectronic sequence. The energy parameters were obtained with Hartree–Fock relativistic calculations. Least-squares parametric calculation has been carried out to study the fit between experimental and theoretical values.
© 2006 Elsevier Ltd. All rights reserved.

1. Introduction

Palladium-like xenon, Xe IX, has a closed $4d^{10}$ shell in its ground state. Data for higher members of the Pd I sequence are important for achieving the laser action at shorter wavelengths, and laser effect was demonstrated for Xe IX at the wavelength of 418, 1 Å [1]. Resonant transitions against the $4d^9(np + n'f)$ configurations were studied in the Pd I isoelectronic sequence from Cd III to Cs X by Churilov et al. [2], and also in [3].

The spectra of Cd III, In IV, and Sn V, were studied by Joshi and van Kleef [4,5], and the previous studies on Sb VI and Te VII [6] were revised and extended, including I VIII, by Churilov et al. [7], and Xe IX [8,9]. Recent analysis of the Cs X–Ce XIII, and Pr XIV–Nd XV [10,11] has been published.

Spectroscopic data from rare gases can be used in studies related with collision physics, photoelectron spectroscopy, fusion diagnostic, and as mentioned, in laser physics. For a better understanding of the eight times ionized xenon atomic structure, the present investigation was undertaken to study the $4d^9 6s$ configuration of the Xe IX ion, and all energy levels belonging to this configuration were determined by $4d^9 5p$–$4d^9 6s$ transitions.

*Corresponding author. Tel.: + 54 221 4840280; fax: + 54 221 4712771.

E-mail addresses: monicar@ciop.unlp.edu.ar (M. Raineri), jreyna@ciop.unlp.edu.ar (J.G. Reyna Almandos).

The spectral analysis was supported by theoretical calculation using the Cowan codes [12] and by means of least squares fits along the Pd I sequence for the $4d^9 6s$ configuration [7]. For this configuration we also extrapolated accurate energy level values along the isoelectronic sequence, using the multiconfiguration Dirac Fock (MCDF) method [13], and Hartree–Fock relativistic calculations [12].

2. Experimental

To excite the xenon spectra we used a capillary pulsed discharge that is a Pyrex tube, 100 cm long, and with an inner diameter of 0.3 cm. The electrodes, placed 80 cm apart, were made of tungsten covered with indium, this one, used to avoid the impurities coming from the electrodes. At one side of the tube there is an inlet connected via a pressure reduction system to the bottle of xenon. In this way a continuous flow of gas was achieved during the exposures.

Gas excitation is produced by discharging a bank of low-inductance capacitors of 240 nF and charged up to 19 kV through the tube. The gas pressure was measured by a thermocouple vacuum gauge before and after the exposures. The pressure range was varied between 5 and 150 mTorr. Light emitted axially was analysed using a 3 m normal incidence vacuum spectrograph with a concave diffraction grating with 1200 lines/mm, blazed for 1200 Å, with plate factor 2.77 Å/mm in the first diffraction order. Ilford Q-2 and Kodak SWR plates were used to record the spectra. Known lines of Xe and C, N, O, were used as internal wavelength standards.

The wavelength values of the measured lines are estimated to be correct to ± 0.02 Å. The intensities figures are visual estimates of photographic density, and are on a uniform scale only within limited wavelength ranges. To distinguish among different states of ionization, we studied the behaviour of the spectral lines intensity as a function of pressure.

3. Results and discussion

Theoretical predictions were used in the analysis of the spectra. To obtain these predicted energy level values and the transition probabilities from de Cowan computer codes [12], we included into calculation the even $4d^{10}$, $4d^9$ ns (n = 5, 6), $4d^9$ nd (n = 5, 6), $4d^8$ $5s^2$, $4d^8$ $5s5d$, $4d^8$ $5d^2$, $4p^5$ $5d^{10}$ 5p and $4p^5$ $5d^{10}$ nf (n = 4, 5) configurations and the odd $4d^9$ np (n = 5, 6), $4d^9$ nf (n = 4 − 6), $4d^8$ $5s5p$, $4d^8$ $5p5d$, $4d^8$ 5s nf (n = 4, 5), $4p^5$ $4d^{10}$ 5s and $4p^5$ $4d^{10}$ 5d configurations. The radial parameters were scaled to 0.85 of their ab initio Hartree–Fock values.

The transitions observed in the present investigation are listed in Table 1. They are shown as combinations between energy levels of the $4d^9 6s$ configuration, against levels of the $4d^9 5p$ configuration, taken from the work of Churilov et al. [9]. The intensities of the observed lines, marked by Int. in the table, are based on visual estimates and the wavenumber values given in the calculated column are deduced from the optimized level values. The level values were determined in a procedure where the wavenumbers of the observed lines are weighted according to their estimated uncertainties. We also presented in this table the calculated transition probabilities (gA, where g is the statistical weight of the upper level and A, the Einstein coefficient for spontaneous emission).

Theoretical calculations along the isoelectronic sequence were also made using the MCDF code of Grant [13]. We also use the predicted MCDF and HFR [12,13] energy levels together the reported experimental $4d^9 6s$ energy levels in the sequence, to help us in the search of the energy levels. Studying the behaviour of the difference between the observed and calculated energies along the isoelectronic sequence and using the energy of $^3D_3$ as reference value, we established all the extrapolated energy level values of the configuration. Fig. 1 shows the $^3D_1$–$^3D_3$ and $^3D_2$–$^3D_3$ energy level differences using E_{obs}–E_{cal} (HFR) values, along the isoelectronic sequence.

Table 2 shows the experimental energy level values of the $4d^9$ 6s configuration and the percentage composition of the $4d^9 6s$ energy levels in L–S coupling. The designation of the levels $^1D_2$ and $^3D_2$ is a little ambiguous. The contribution to the $^3D_2$ level is 54% ^3D and 46% ^1D. The same fact can be seen with these levels in other ions belonging to the isoelectronic sequence.

To give the best possible fit between the calculated eigenvalues and the observed energy levels, the radial integrals E_{av}, F^k, G^k, ζ and R^k were considered as adjustable parameters, whose values were determined considering their behaviour through the isoelectronic sequence. The accuracy of the fit is measured by means of the standard deviation in a least-squares calculation [12].

Table 1
Classified lines in the $4d^9 5p$–$4d^9 6s$ transitions in Xe IX

gA^a	Int.	Wavelengths λ (Å)	Wavenumber		Classification
			σ_{obs} (cm^{-1})	σ_{cal} (cm^{-1})	
57	2	306.52	326 243	326 248	5p $^3P_2$–6s $^3D_3$
33	1	307.50	325 203	325 192	5p $^3F_2$–6s $^3D_1$
18	1	308.02	324 650	323 654	5p $^3P_1$–6s $^3D_2$
0.1	1	308.80^b	323 834	324 824	5p $^3P_1$–6s $^3D_1$
0.3	1	308.80^b	323 834	323 824	5p $^3F_3$–6s $^1D_2$
27	1	309.88	322 706	322 700	5p $^3F_3$–6s $^3D_3$
15	1	318.15	314 317	314 299	5p $^1P_1$–6s $^3D_2$
10	1	322.10	310 463	310 440	5p $^3P_0$–6s $^3D_1$
14	1	324.38	308 282	308 288	5p $^3P_1$–6s $^1D_2$
92	3	328.04	304 841	304 832	5p $^3F_4$–6s $^3D_3$
68	3	330.03	303 003	303 019	5p $^1F_3$–6s $^3D_2$
41	2	333.05	300 255	300 269	5p $^1D_2$–6s $^1D_2$
24	1	333.27	300 057	300 077	5p $^3D_1$–6s $^3D_1$
30	1	335.53	298 032	298 029	5p $^3D_2$–6s $^3D_2$
21	1	336.24	297 411	297 400	5p $^3D_3$–6s $^1D_2$
17	1	336.51	297 168	297 199	5p $^3D_2$–6s $^3D_1$
42	1	337.53	296 270	296 276	5p $^3D_3$–6s $^3D_3$

^{a}Calculated gA values (given in the 10^9 s^{-1} units) where g stands for statistical weight of the transition upper level and A, for Einstein's coefficient for spontaneous emission.
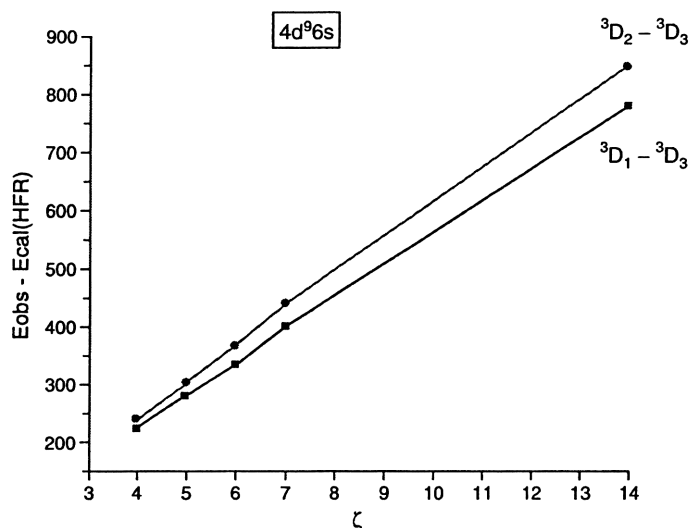
^{b}Double classification.

Fig. 1. $^3D_1$–$^3D_3$ and $^3D_2$–$^3D_3$ energy level differences using E_{obs}–E_{cal} (HFR) values, along the isoelectronic sequence.

Table 3 shows the energy parameters for the $4d^{10}$, $4d^9$ 5s, 6s and $4d^9$ 5d configurations of Xe IX. All the parameters are free except the configuration interaction integrals which were fixed at 0.85 of their Hartree–Fock value. The average parameter deviations of the fits are also given in this table. The Fit/HF parameter ratios for the ζ_{4d} and $G^2(4d,6s)$ of the $4d^9$ 6s configuration are in accordance with the scaled factor of the isoelectronic sequence [7]. The configuration interaction integral for the $4d^9$ 6s configuration are not significant with respect to the other interactions involved in the calculation. The standard deviation of the least squares fit of the observed levels is 85 cm^{-1}.

Table 2

New energy level values of the $4d^9 6s$ configuration of Xe IX

Designation	E_{exp} (cm^{-1})	E_{calc} (cm^{-1})[a]	Percentage composition
$^3D_1$	918 346	918 340	100 ^3D
$^3D_2$	919 176	919 178	54 $^3D_2$ + 46 $^1D_2$
$^3D_3$	901 686	901 685	100 ^3D
$^1D_2$	902 810	902 801	54 $^1D_2$ + 46 $^3D_2$

[a]Calculated energy level values obtained using the fitted energy parameters.

Table 3

Energy parameters for the $4d^{10}$, $4d^9 5s$, $4d^9 6s$ and $4d^9 5d$ configurations of Xe IX

Configuration	Parameter	H–F value	Fitted value	Fitt/H–F
$4d^{10}$	E_{av}	0	1482	
$4d^9 5s$	E_{av}	465 886	461 992 ± 44	0.99
	ζ_{4d}	6397	6614 ± 36	1.03
	G^2 (4d, 5s)	18 847	16 922 ± 416	0.90
$4d^9 6s$	E_{av}	908 208	908 853 ± 43	1.00
	ζ_{4d}	6447	6663 ± 34	1.03
	G^2 (4d, 6s)	5128	4797 ± 425	0.93
$4d^9 5d$	E_{av}	799 545	799 392 ± 24	1.00
	ζ_{4d}	6439	6635 ± 19	1.03
	ζ_{5d}	1181	1389 ± 27	1.17
	F^2 (4d, 5d)	32 600	28 716 ± 356	0.88
	F^4 (4d, 5d)	15 408	14 918 ± 565	0.97
	G^0 (4d, 5d)	7692	6103 ± 28	0.79
	G^2 (4d, 5d)	9742	8930 ± 242	0.92
	G^4 (4d, 5d)	8195	7438 ± 544	0.91
Configuration interaction integrals				
$4d^{10}$–$4d^9 5s$	R^2 (4d4d, 4d5s)	−7893	−6709 (FIX)	0.85
$4d^{10}$–$4d^9 6s$	R^2 (4d4d, 4d6s)	−5348	4546 (FIX)	0.85
$4d^{10}$–$4d^9 5d$	R^0 (4d4d, 4d5d)	2284	1942 (FIX)	0.85
$4d^{10}$–$4d^9 5d$	R^2 (4d4d, 4d5d)	17 038	14 483 (FIX)	0.85
$4d^{10}$–$4d^9 5d$	R^4 (4d4d, 4d5d)	13 162	11 188 (FIX)	0.85
$4d^9 5s$–$4d^9 6s$	R^2 (4d5s, 6s4d)	9287	7894 (FIX)	0.85
$4d^9 5s$–$4d^9 5d$	R^2 (4d5s, 4d5d)	35 703	30 348 (FIX)	0.85
$4d^9 5s$–$4d^9 5d$	R^2 (4d5s, 5d4d)	10 134	8614 (FIX)	0.85
$4d^9 6s$–$4d^9 5d$	R^2 (4d6s, 4d5d)	5680	4828	0.85
$4d^9 6s$–$4d^9 5d$	R^2 (4d6s, 5d4d)	4335	3685	0.85

The standard deviation of the fit is 85 cm^{-1} for 26 observed levels.

Acknowledgments

References

[1] Lemoff BE, Yin GY, Gordon III CL, Barty CPJ, Harris SE. J Opt Soc Am B 1996;13:180–4.
[2] Churilov SS, Joshi YN, Ryabtsev AN. J Phys B 1994;27:5485–95.
[3] Churilov SS, Joshi YN. Phys Scr 2002;65:40–5.

[4] van Kleef ThAM, Joshi YN, Uijlings P. Phys Scr 1980;22:353–62.

[5] van Kleef ThAM, Joshi YN. Phys Scr 1981;24:557–65.

[6] Joshi YN, van Kleef ThAM. Can J Phys 1979;57:1982–9.

[7] Churilov SS, Azarov VI, Ryabtsev AN, Tchang-Brillet W-ÜL, Wyart J-F. Phys Scr 2000;61:420–30.

[8] Ryabtsev AN, Antsiferov PS, Nazarenko AV, Churilov SS, Tchang-Brillet Ü-L, Wyart J-F. J Phys IV 2001;Pr2:317–9.

[9] Churilov SS, Ryabtsev AN, Tchang-Brillet W-ÜL, Wyart JF. Phys Scr 2002;66:293–307.

[10] Churilov SS, Ryabtsev AN, Tchang-Brillet W-ÜL, Wyart J-F. Phys Scr 2002;T100:98–103.

[11] Churilov SS, Ryabtsev AN, Wyart J-F, Tchang-Brillet W-ÜL, Joshi YN. Phys Scr 2005;71:589–98.

[12] Cowan RD. The theory of atomic structure and spectra. Berkeley, CA: University of California Press; 1981.

[13] Grant IP, Mc Kenzie BJ, Norrington PH, Mayers DF, Pyper NC. Comput Phys Commun 1980;21:207–31;
McKenzie BJ, Grant IP, Norrington PH. Comput Phys Commun 1980;21:233–46.